NRL Release Number 04-1226-1873

Estimation of Fringe Parameters

D. Mozurkewich[a], J. T. Armstrong[b], G. C. Gilbreath[b], T. A. Pauls[b]

[a]Seabrook Engineering, 9310 Dubarry Ave, Seabrook MD, 20706 USA;
[b]US Naval Research Laboratory, 4555 Overlook Ave SW, Washington DC, 20475 USA

ABSTRACT

In this report we explore replacing the widely used optimal V^2 estimator with a model-fitting approach. We show that it is possible to fit the fringe power spectra with a physically reasonable model. This approach eliminates the biggest problem with the standard squared visibility estimator – determining the additive, detector-noise bias. We examine the dependence of the bias on count rate for consistency between on- and off-fringe measurements. The change of bias with fringe frequency provides additional information about the performance of the detectors. We have also applied a similar approach to the bias correction for the triple product, with comparable results.

Keywords: Long Baseline Optical Interferometry, Data Reduction

1. INTRODUCTION

The optical interferometers with heritage tracing back to the Mark III[1] are fringe tracking interferometers in the sense that data is only taken while reasonably centered on the fringe packet and the data rate is fast compared to the atmospheric coherence time. The data consists of intensity measurements versus delay where the delay range is small compared to the width of the fringe packet. Since optimum fringe parameter estimators have long been known for this regime,[2,3] the data reduction problem is considered a solved problem; the challenge is to estimate the bias terms[4,5] that appear in those equations. The bias corrections usually include observing the star off the fringe (hereafter called off-fringe scans) and can consume as much as 50% of the on star integration time.

An alternative approach, adopted by most of the other optical interferometers, consists of fitting a model, which includes the fringe parameters, directly to the raw data. Although it is always a good idea to measure what it is you want to know, the converse of fitting what you want to know directly to what you measure is not always appropriate; when there is so much data that the deviation of the mean is orders of magnitude smaller than the standard deviation, it can be difficult separating systematics in the data or omissions in the model from a lack of a precise knowledge of the data uncertainties.

In this paper, we explore a model fitting approach, but fitting to intermediate data products. Instead of calculating the bias and then using the standard V^2 estimator, we fit a model to the fringe power spectrum to determine both the squared visibilities and the bias. Such an approach provides a way to account for the real physical characteristics of the fringe detection process that make the standard optical estimator difficult to use. In the NPOI data used as an example here, effects associated with afterpulsing, dead time and cross-talk are clearly visible, and they can be used to assess the performance of the system. As an added benefit, the need for off-fringe measurements can be substantially reduced or even eliminated providing as much as a factor of two improvement in throughput. Similarly, the triple product can be replaced with the bispectrum with equally promising results.

E-mail: dave@mozurkewich.com,tom.armstrong@nrl.navy.mil,Charmaine.Gilbreath@nrl.navy.mil,pauls@nrl.navy.mil

New Frontiers in Stellar Interferometry, edited by Wesley A. Traub,
Proceedings of SPIE Vol. 5491 (SPIE, Bellingham, WA, 2004)
0277-786X/04/$15 · doi: 10.1117/12.552416

2. SQUARED VISIBILITY AMPLITUDES

The fundamental data consist of N evenly-spaced measurements distributed over ℓ wavelengths of delay. For the NPOI, $N = 64$ and for the data shown here, ℓ takes on the values of 2, 4 or 6 depending on the baseline. For PTI and the Keck interferometer, $N = 4$ but that value can be increased with no loss of sensitivity. The standard squared visibility estimator, V_ℓ^2, is given by

$$V^2(\ell) = 4\frac{\langle F(\ell)F^*(\ell) - \sigma^2(I_0)\rangle}{\langle I_0\rangle^2}, \tag{1}$$

where $F(k)$ is the Fourier Transform of the bin counts, I_0 is the total number of counts and $\sigma^2(I_0)$ is a bias correction. We ignore the frequency dependent reduction in V^2 due to finite sampling size. This oft-quoted form of the bias correction is valid only when the variance is linearly dependent on the count rate.

We start our model fitting by calculating the fringe power spectrum, $P(k) = \langle F(k)F^*(k)\rangle$ as a function of fringe frequency for all possible frequencies. The model used to fit these data is

$$P(k) = P_0 + \frac{P_1}{1 + (t_0 k)^2} + \sum_\ell \frac{V_\ell^2 \langle I_0\rangle^2 \mathrm{sinc}^2(\ell - k)}{4}. \tag{2}$$

$P(k)$ and $\langle I_0\rangle$ are measured. The bias corrected squared visibility amplitude, V_ℓ^2 is determined from fitting Equation 2 to these data. A typical result is shown in Figure 1. The bias is simply the value of the noise power spectrum (the first two terms of Equation 2) evaluated at the fringe frequency.

Note that the noise power spectrum is not white. The form adopted for Equation 2 is based on the assumptions that the most important non-white noise is due to afterpulsing and that the afterpulses are distributed exponentially in time after the initiating event. The sinc^2 form for the fringe results from the assumption that we scan across the fringe at a constant rate; departure from a linear stroke will modify that function. Fitting for the fringe frequencies is possible but not entirely straightforward since the sinc^2 function and its first derivative are zero at each measured frequency, while interpolating the power spectrum results in fitting the model to data with correlated noise. On a few nights for which fringe frequencies were fit, the departures from their nominal values were not deemed large enough to be significant.

Although it is encouraging to see that there are no systematic deviations of the model from the data, it is not obvious how significant this result is; since the departure from a white noise spectrum is small, other functional forms for the frequency dependence also work well. It is reassuring to see that the magnitude of the residuals, though perhaps a little large, is close to what is expected. A noise power spectrum has a signal to noise ratio of one. Averaging 15000 spectra, the expected noise in a power spectrum with a mean value of 100 should be $100/\sqrt{15000} = 0.81$, in good agreement with the measured value of 0.9.

It is also important that multiple fits give consistent results. To test this consistency, we examine how the bias depends on count rate. First, Equation 2 was fit to each scan of data during a night. Then the first two terms were used to determine the bias at the chosen frequency. A typical result is shown in Figure 2. Here, the upper panel shows the bias for every scan taken during that night. Open and closed symbols are used to differentiate between off- and on- fringe scans. The line is a quadratic fit through the off-fringe scans. The residuals of the off-fringe scans are shown in the lower panel. The sizes of the error bars are underestimated by perhaps 30 percent since they were determined by dividing the standard deviation of the residuals in the power spectrum fit (Figure 1) by the square root of the number of fringe frequencies (32) instead of by the number of degrees of freedom in the fit (25). The error bars are about a factor of two smaller than the actual random noise in Figure 2. The systematics clearly indicate that a higher order polynomial fit is indicated. A quadratic was adopted because that is the expected form when dead time corrections are included in the model. Poisson statistics with a dead time equal to a fraction τ of the integration time has variance $\sigma^2 = I_0 - 2\tau I_0^2$. Notice that the bias determined from the on-fringe scans is systematically smaller than the bias determined from the off-fringe scans. This is the expected result when the variance varies non-linearly with signal strength as seen in Figure 2. For a linear dependence between the bias and the count rate, the presence of a fringe does not matter

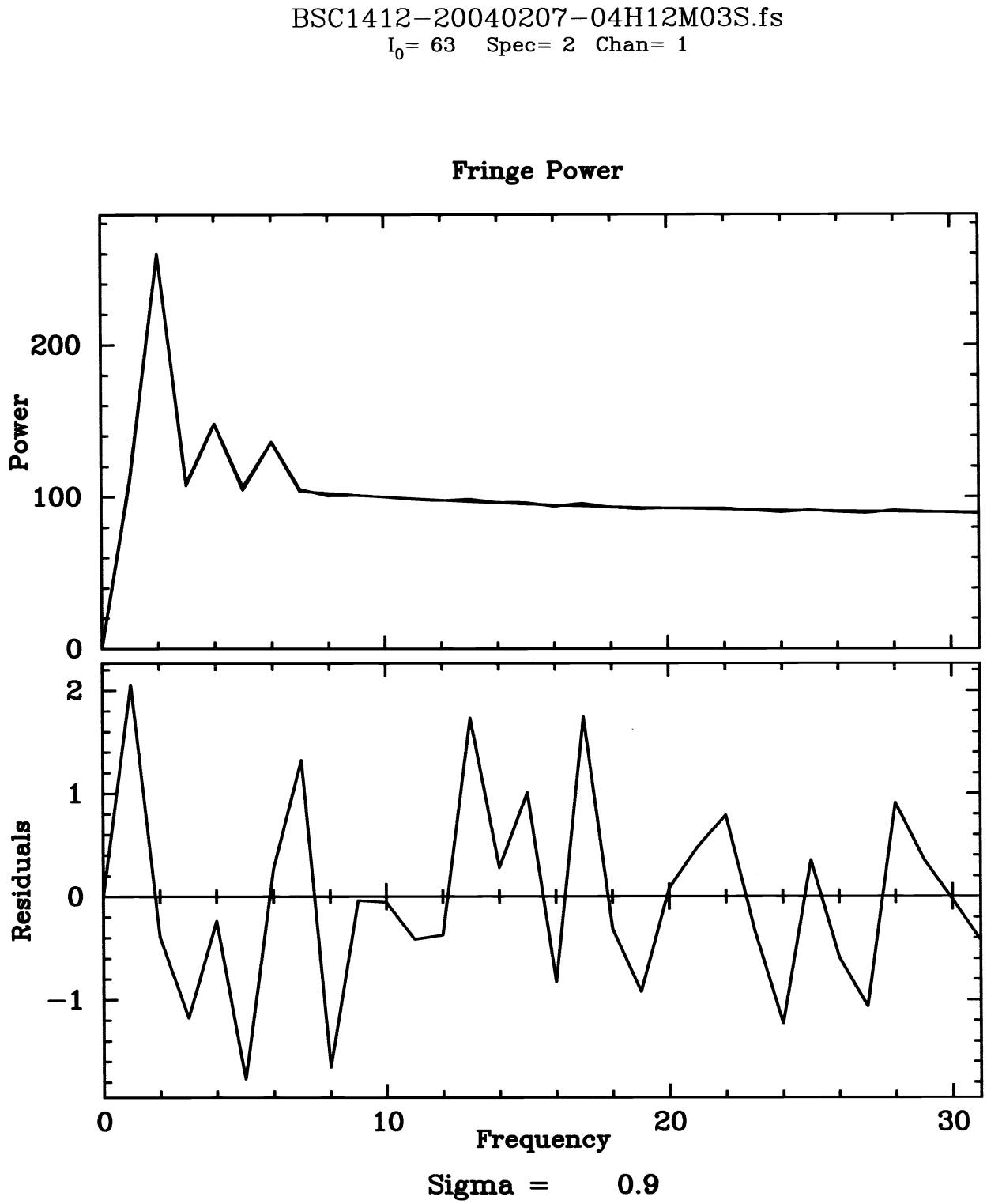

Figure 1. Plot of fringe power versus frequency. The upper panel shows the data and model while the lower panel shows the residuals. This plot is an average of 15000 frames of data.

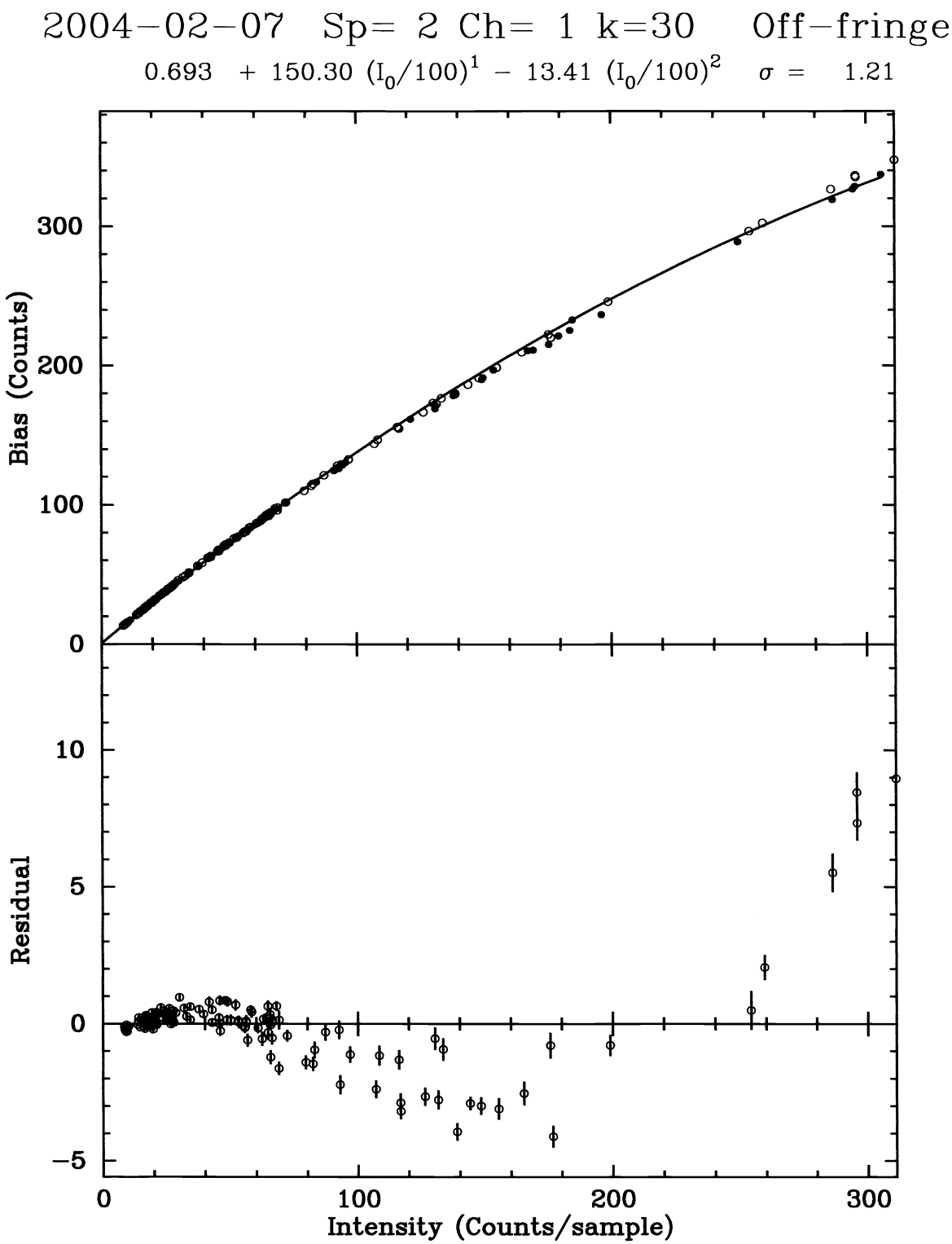

Figure 2. The variation of bias with fringe frequency (top) and the residuals to a fit to the off-fringe data (bottom). Open circles represent off-fringe data; filled circles are on-fringe data. Although a cubic fits the data better, a quadratic was adopted since it results from a non-zero dead time for the photon-counting detectors.

since the mean of the bias (for the individual bins) is equal to the bias of the mean. But if the dependence is quadratic, $\sigma^2 = aI_0 + bI_0^2$, the bias contains an additional term

$$\text{Bias} = \frac{\langle I_0 \rangle^2 b}{4} \sum_{\ell} V_{\ell}^2. \tag{3}$$

Since b is negative, this results in a reduction of the bias correction. Figure 3 shows the same data as in Figure 2 except now residuals for all scans are shown. The fit is still through the off-fringe scans. The open circles again show the off-fringe residuals, the solid circles show the on-fringe residuals. The solid five-pointed stars show the on-fringe residuals with Equation 3 subtracted, that is, the off-fringe bias that is needed to be consistent with the on-fringe measurement. The agreement between the corrected on-fringe bias and the off-fringe bias is acceptable.*

So far, we have only considered the bias at frequencies far removed from the fringes. At frequencies close to the fringes, a somewhat different behavior is observed. Figure 4 shows the bias near the middle of the frequency region populated with baselines. Now, we see the on-fringe scans have systematically *higher* bias. Correcting the biases for the nonlinearity will only make the agreement worse. It is reasonable, although perhaps not necessary, to attribute this offset to cross-talk; a delay modulation that is not exactly the assumed shape and amplitude can "scatter" power into other frequencies. This raises an important philosophical issue: which bias value is correct? When a single baseline is present on the detector, it makes little difference as long as a consistent approach is used. This is because the error in the bias goes to zero as the V^2 goes to zero so that choice of bias does not affect low visibility measurements. For high visibility measurements, the offset can be absorbed into the calibration†. When multiple fringes are present in the data, this is no longer the case since typically some baselines will have low V^2 while for others it is large. In this case, doing the on-fringe bias correction is almost certainly the preferred method. Fortunately for these data, the difference is small; for all cases in this data set the bias offset results in less than a 1% change in the measured V^2. The offset is typically greater than 0.1% so it is significant if high precision is desired.

3. TRIPLE PRODUCTS

The bias correction for triple products can be accomplished in a manner completely analogous to the V^2 bias corrections. The calculation of the triple product is replaced with a calculation of the bispectrum. The bispectrum is defined as

$$B(k_1, k_2) = F(k_1)F(k_2)F^*(k_1 + k_2). \tag{4}$$

When two baselines of a triangle are at fringe frequencies k_1 and k_2, the third baseline (with the wrong sign) is at frequency $k_1 + k_2$. Therefore the phase of the bispectrum at k_1, k_2 is equal to the closure phase of that triangle. The bispectrum at other frequency pairs can be used to estimate the bias. An example of the bispectrum is shown in Figures 5. The bispectrum is symmetric around the $k_1 = k_2$ line so that this plot shows twice as much data as necessary. There are two important points here. First, the bias is only in the real part of the bispectrum. By not properly accounting for the bias, the closure phases are biased toward (or away from) zero. This is a particularly insidious effect because it cannot be detected by observing point sources. A second problem is the bands that occur when one of the frequencies corresponds to a baseline. Since these bands pass through the peaks of interest, they can account for a significant amount of the bias and since they disappear in the off-fringe scans, they cannot be calibrated by calculating only the triple products. The simplest functional form for the bispectrum bias that seems to work is

$$\begin{aligned} B(k_1, k_2) &= B_0 + B_1 \left[\frac{1}{1 + (t_0 k_1)^2} + \frac{1}{1 + (t_0 k_2)^2} + \frac{1}{1 + t_0 (k_1 + k_2)^2} \right] \\ &+ \sum_k D_k [\text{sinc}(k_1 - k) + \text{sinc}(k_2 - k) + \text{sinc}(k_1 + k_2 - k)] \end{aligned} \tag{5}$$

*In the interest of full disclosure, we note that the detector selected for these plots is the one with the largest nonlinearity. For the other detectors, the offset is generally smaller and the nonlinearity correction does not account for the entire offset. An effort to determine a more complete understanding of these effects is underway.

†We use the term *bias* to refer to an additive offset between the observed and actual V^2 and the term *calibration* to refer to a multiplicative offset.

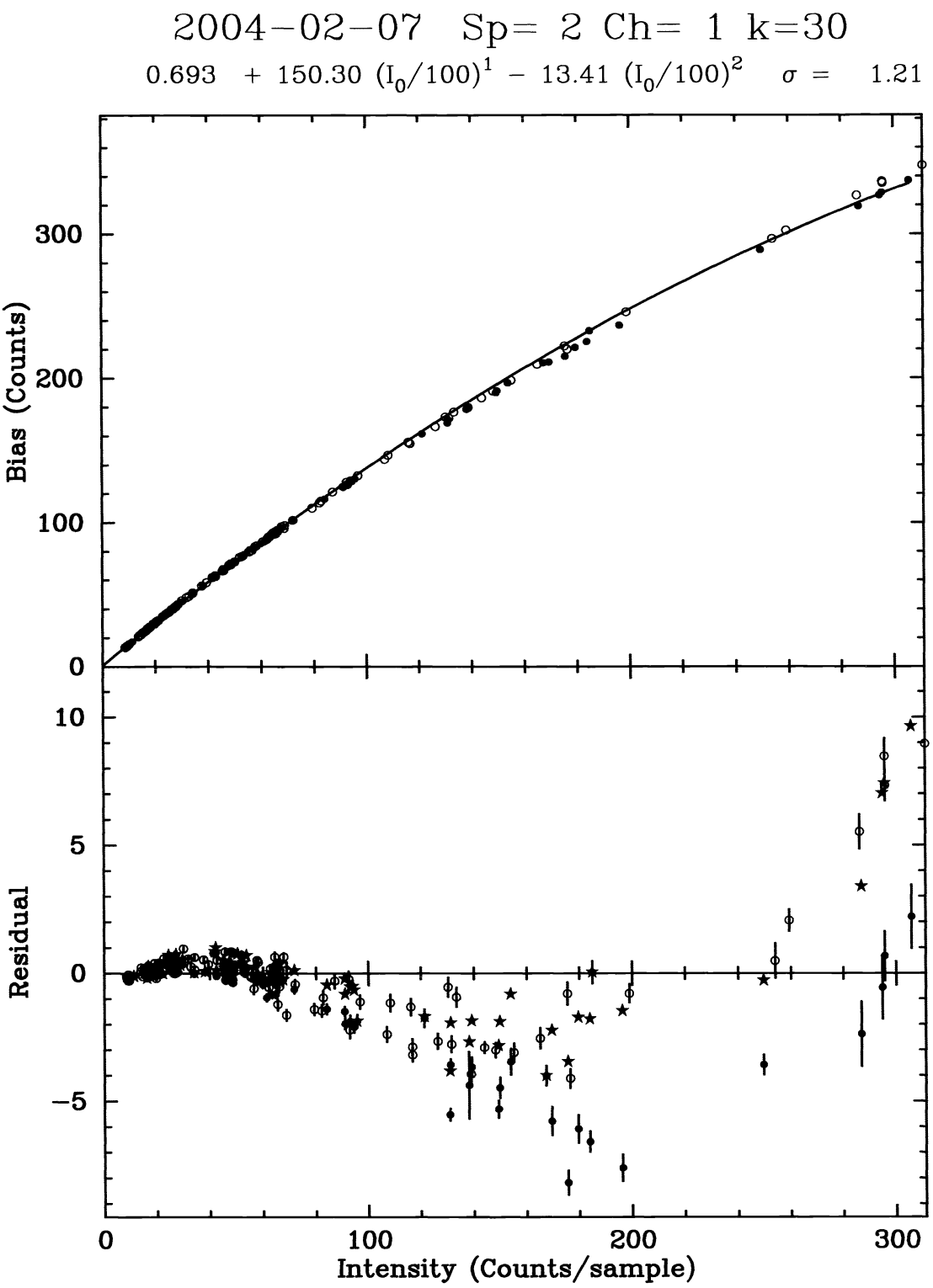

Figure 3. The same as Figure 2 except the residuals for all scans are shown. The stars show on-fringe data corrected for the non-linear variance (Equation 3). Notice that the residuals for the on-fringe scans are systematically offset from the residuals determined by the off-fringe scans. The offset between the solid stars and solid circles show the magnitude of the offset due to the non-linearity. If the entire offset between the on- and off-fringe scans is accounted for by this effect, the stars should line up with the off-fringe scans (open circles).

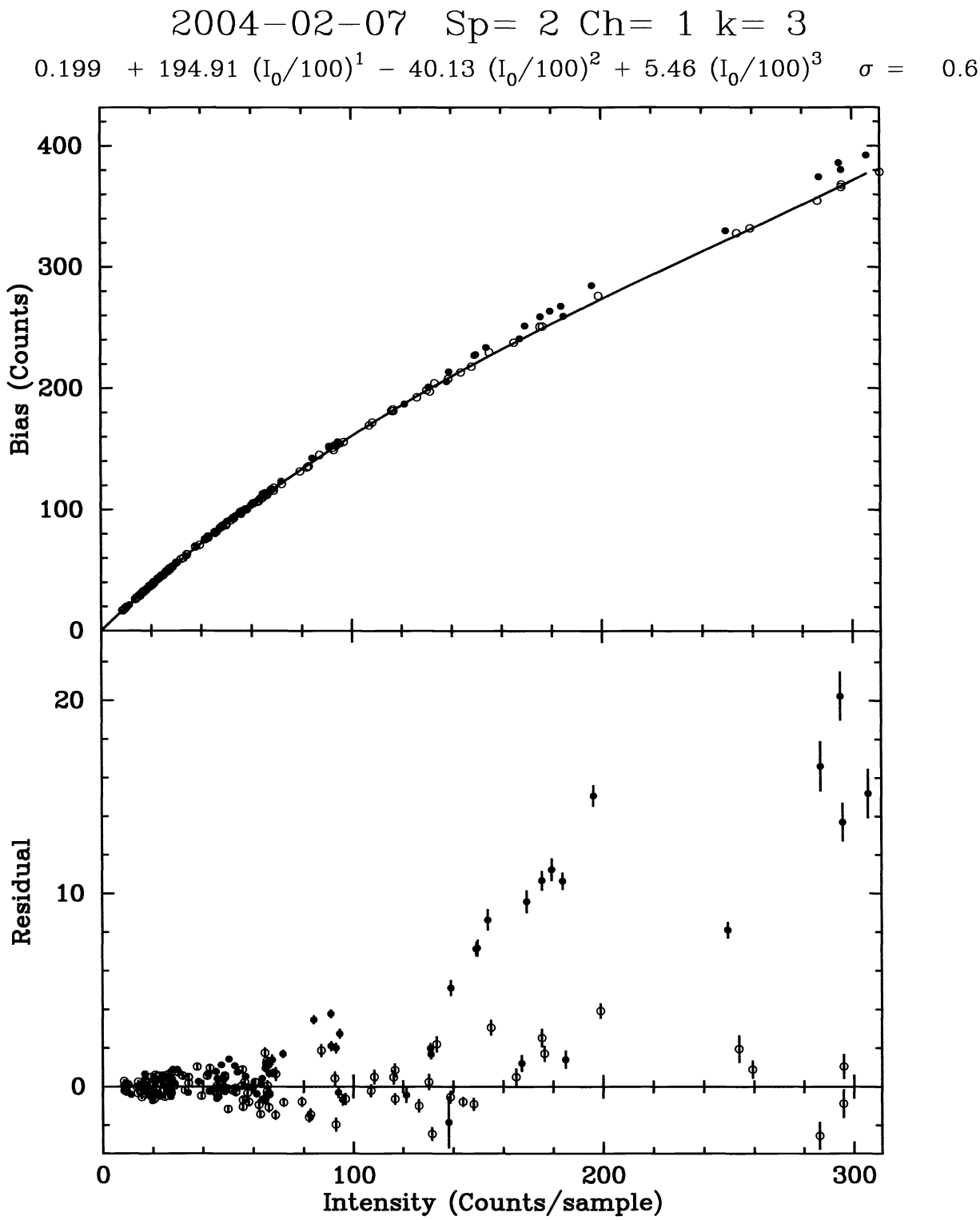

Figure 4. The same as Figure 3 except for a frequency near the fringes. Now the on-fringe scans require a consistently larger bias correction. Although statistically significant, the difference in bias between the on- and off-fringe scans is small, corresponding to an error in V^2 of a couple parts per thousand.

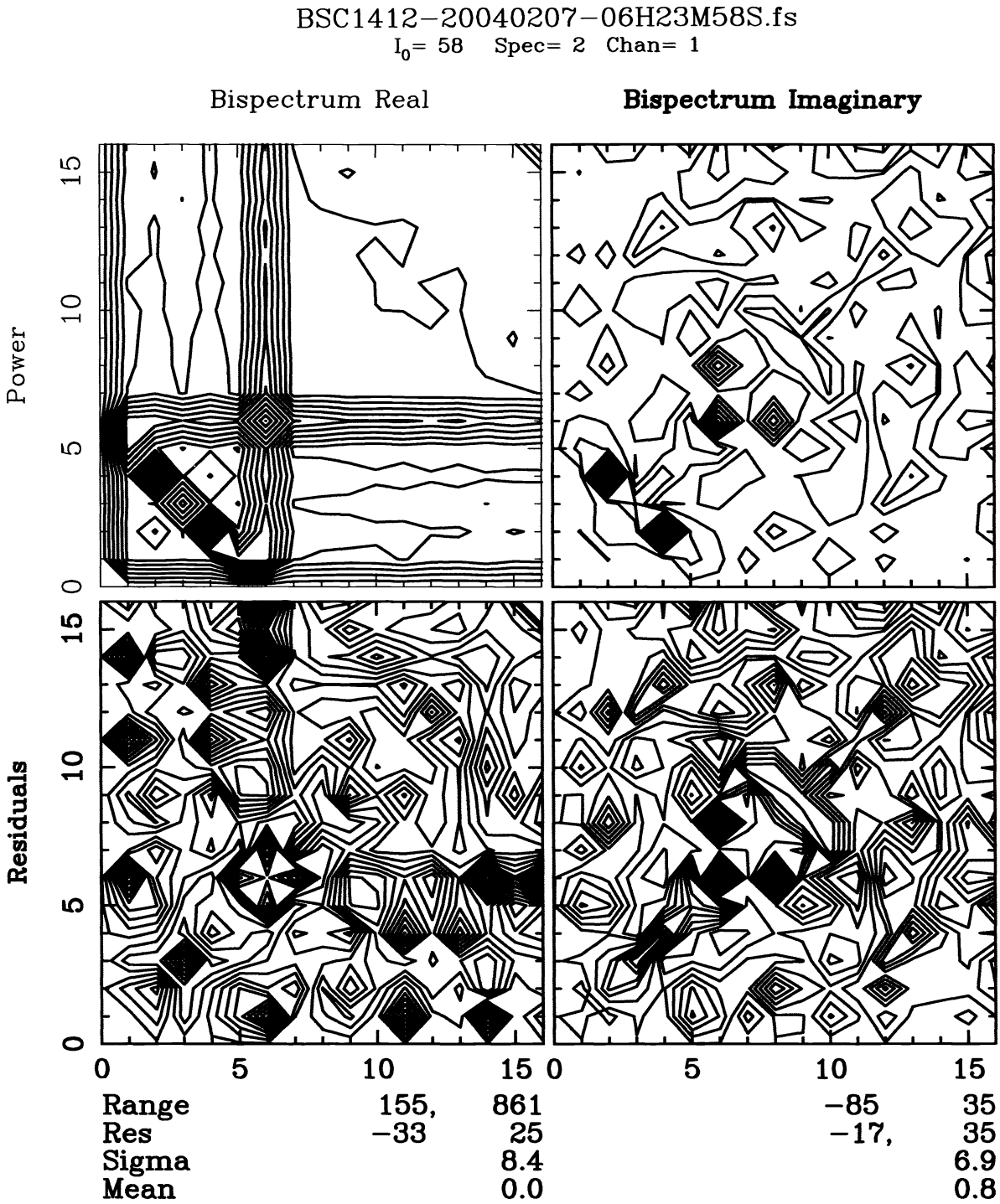

Figure 5. Contour plots of the bispectrum. The real part is on the left, the imaginary part on the right. The top and bottom rows show the raw data and the residual to a fit, respectively. The axes are the fringe frequency, k, in cycles. The fringes are at $k = 2$, 4 and 6 and form a single triangle. The real part has a bias consisting of a smooth background, decreasing in value toward the upper right. Each fringe present in the data also contributes to the bias with vertical and horizontal bands at the fringe frequency and with a diagonal band running from $(0, k)$ to $(k, 0)$. The real part of the triple product is the value of the bispectrum at $(2, 4)$, corrected for this bias. The imaginary part of the bispectrum is unbiased.

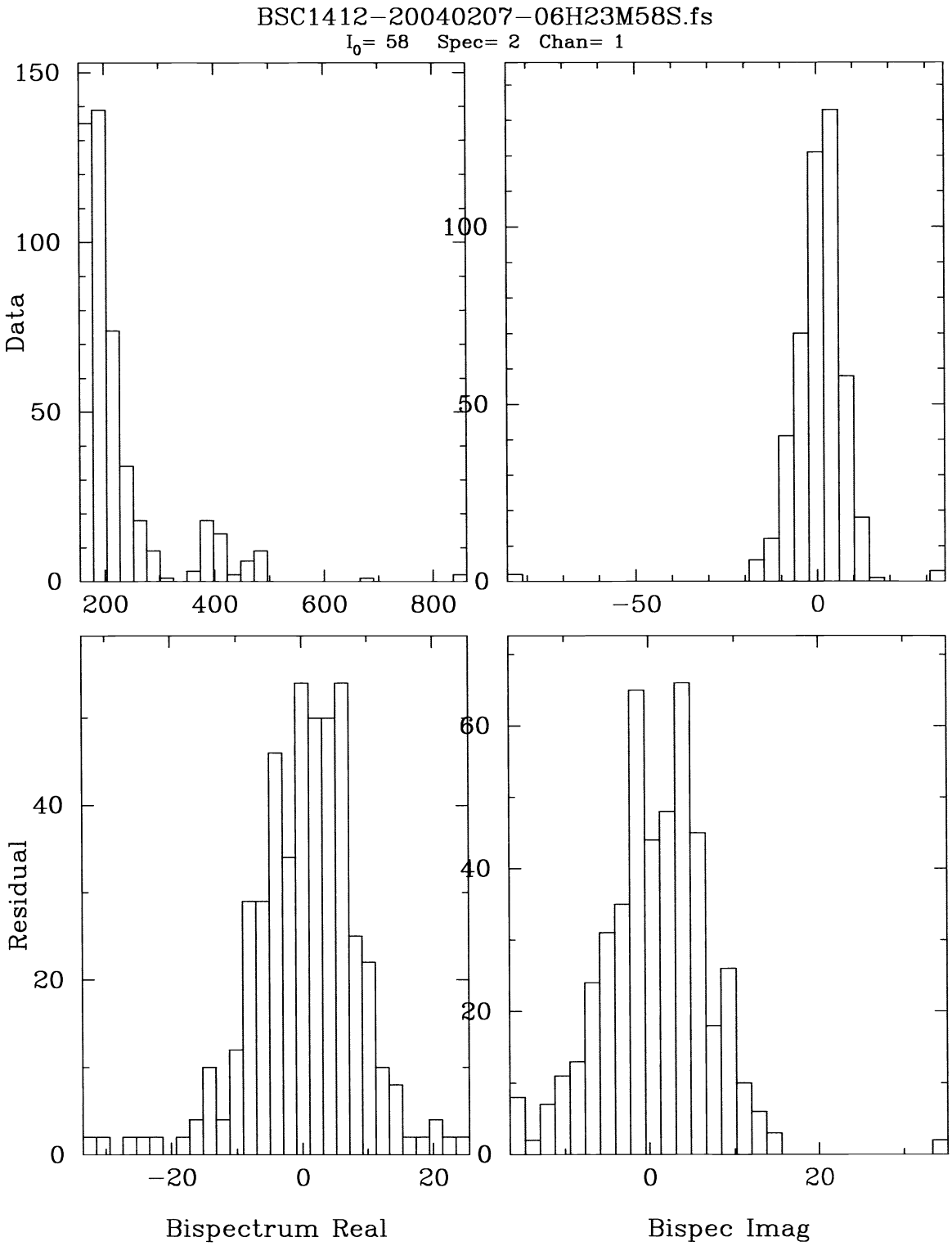

Figure 6. The histogram of the data shown in Figure 5. The upper panels show the raw data; the low panels the residuals of the data from the fit. The symmetric, zero mean distributions of residuals imply the fits are good.

where B_0, B_1, t_0 and one D_k for each fringe present in the data are free parameters. The results of the fit are shown in Figure 6. The symmetric, zero-mean residuals imply that the model is sufficient.

4. SUMMARY

Use can be made of model-fitting power spectrum to determine bias corrections. This is both more accurate and more precise than the use of off-fringe scans. The use of off-fringe scans can be eliminated allowing a full factor of two improvement in throughput. Note that the use of a large number of fringes is not restricted to photon-counting detectors; any detector that allows non-destructive reads, such as those used for the Keck Interferometer, can be used with this technique.

Bias corrections for triple products need only be applied to the real part. This biases the phase either toward or away from zero. Since observations of point sources have zero closure phase, they cannot be used to assess their correctness.

ACKNOWLEDGMENTS

The research was supported by the the Office of Naval Research.

REFERENCES

1. M. Shao, M. M. Colavita, B. E. Hines, D. H. Staelin, D. J. Hutter, K. J. Johnston, D. Mozurkewich, R. S. Simon, J. L. Hershey, J. A. Hughes, and G. H. Kaplan, "The Mark III Stellar Interferometer," *Astron and Astrophys* **193**, p. 357, 1988.
2. W. J. Tango and R. Q. Twiss in *Progress in Optics, XVII*, E. Wolf, ed., p. 239, North-Holland, Amsterdam, 1980.
3. B. Wirnitzer, "Bispectral analysis at low light levels and astronomical speckle masking," *JOSA A* **2**, p. 14, 1985.
4. M. M. Colavita, "Fringe visibility estimators for the Palomar Testbed Interferometer," *Pub. Astron. Soc. of the Pacific* **111**, pp. 111–117, 1999.
5. M. Wittkowski, C. A. Hummel, K. J. Johnston, D. Mozurkewich, A. R. Hajian, and N. M. White, "Direct multi-wavelength limb-darkening measurements of three late-type giants with the Navy Prototype Optical Interferometer," *Astron. and Astrophys.* **377**, p. 981, 2001.